THE JOURNAL OF PHYSICAL CHEMISTRY Letters

Perspective

pubs.acs.org/JPCL

Recent Progress in the Functionalization Methods of Thiolate-Protected Gold Clusters

Wataru Kurashige,[†] Yoshiki Niihori,[†] Sachil Sharma,[†] and Yuichi Negishi*[,†,‡,#]

[†]Department of Applied Chemistry, Faculty of Science, Tokyo University of Science, 1-3 Kagurazaka, Shinjuku-ku, Tokyo 162-8601, Japan

[‡]Photocatalysis International Research Center, Tokyo University of Science, 2641 Yamazaki, Noda, Chiba 278-8510, Japan

[#]Department of Materials Molecular Science, Institute for Molecular Science, Myodaiji, Okazaki, Aichi 444-8585, Japan

ABSTRACT: Nanomaterials that exhibit both stability and functionality are currently considered to hold great promise as components of nanotechnology devices. Thiolate-protected gold clusters ($Au_n(SR)_m$) have long attracted attention as functional nanomaterials. Magic $Au_n(SR)_m$ clusters are an especially stable group of thiolate-protected clusters that have particularly high potential as functional materials. Although numerous application experiments have been conducted for magic $Au_n(SR)_m$ clusters, it is important that functionalization methods are also established to allow for effective utilization of these materials. The results of recent research on heteroatom doping and the use of other chalcogenide ligands strongly suggest that these strategies are promising as functionalization methods of magic $Au_n(SR)_m$ clusters. In this Perspective, we focus on studies relating to three representative types of magic clusters—$Au_{25}(SR)_{18}$, $Au_{38}(SR)_{24}$, and $Au_{144}(SR)_{60}$—and discuss the recent progress and future issues.

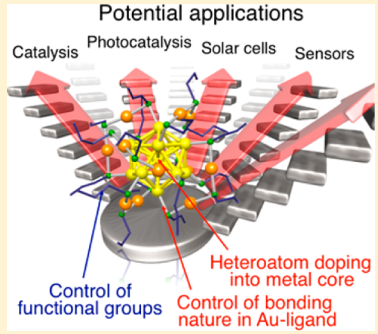

Nanotechnology is expected to solve a broad range of problems in many fields, including materials science, energy, the environment, healthcare, and information communications. However, to achieve dramatic advances with this type of technology, there is a strong need for the creation of stable, highly functional nanomaterials.

> To effectively use magic $Au_n(SR)_m$ clusters in various fields, it is important that functionalization methods are established for magic $Au_n(SR)_m$ clusters in addition to studying their applications.

Thiolate-protected gold clusters ($Au_n(SR)_m$; Figure 1)[1] possess a strong bond between metal and thiolate and are therefore very stable against degradation in both solution and the solid state. These clusters also exhibit size-specific properties that are not observed in bulk metals, such as photoluminescence,[2−7] redox behavior,[4] and catalytic activity.[8] Because of these properties, $Au_n(SR)_m$ clusters have attracted considerable attention as functional nanomaterials for many years. Magic $Au_n(SR)_m$ clusters are an especially stable type of $Au_n(SR)_m$ clusters that have particularly high potential as functional materials. Examples of representative magic $Au_n(SR)_m$ clusters include $Au_{25}(SR)_{18}$ (refs 9−17), $Au_{38}(SR)_{24}$ (refs 18−20), and $Au_{144}(SR)_{60}$ (refs 21−24) (Figure 1). These clusters are stabilized by geometrical factors,

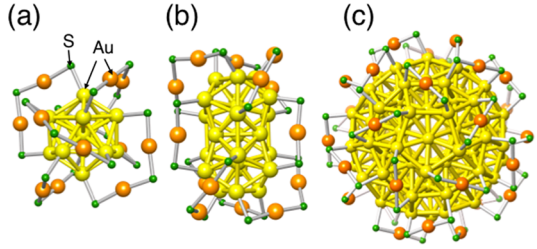

Figure 1. Geometrical structures of representative magic $Au_n(SR)_m$ clusters: (a) $Au_{25}(SR)_{18}$ (refs 11−13), (b) $Au_{38}(SR)_{24}$ (ref 19), and (c) $Au_{144}(SR)_{60}$ (refs 22 and 23). The R groups have been omitted for simplicity. $Au_{25}(SR)_{18}$ has a structure in which six $-S(R)[-Au-S(R)-]_2$ oligomers cover an icosahedral Au_{13} core.[11−13] $Au_{38}(SR)_{24}$ has a structure in which nine $-S(R)[-Au-S(R)-]_x$ (x = 1 or 2) oligomers cover a Au_{23} core, which consists of two linked icosahedral Au_{13} groups.[19] $Au_{144}(SR)_{60}$ is proposed to have a structure in which multiple $-S(R)-Au-S(R)-$ oligomers cover a metal core (Au_{84}).[22,23] The figures are adapted from refs 12, 19, and 22.

and $Au_{25}(SR)_{18}$ and $Au_{38}(SR)_{24}$ are further stabilized by electronic factors.[25,26] Because of their high stability, magic $Au_n(SR)_m$ clusters can be synthesized size-selectively with atomic precision. Magic $Au_n(SR)_m$ clusters possessing these characteristics have attracted considerable attention as functional nanomaterials, and research toward the application of their unique physical and chemical properties is currently being performed in numerous fields, including catalysis,[8,27−30]

Received: September 13, 2014
Accepted: November 13, 2014

   dx.doi.org/10.1021/jz501941p | J. Phys. Chem. Lett. 2014, 5, 4134−4142

photocatalysis,[31,32] solar cells,[33,34] fuel cells,[35] sensors,[36] and photosensitizers.[37]

In addition to studying potential applications, functionalization methods should also be studied to effectively use this type of material. The establishment of methods to impart new functions would enable magic $Au_n(SR)_m$ clusters to be converted into more functional and useful nanomaterials. If various types of functionalization methods can be established, stable nanomaterials with desired functions for specific applications could be created by applying these methods to magic $Au_n(SR)_m$ clusters.

To change the functions of these clusters for specific applications, methods involving the control of the functional groups of the ligand are mainly used (Figure 2). For example,

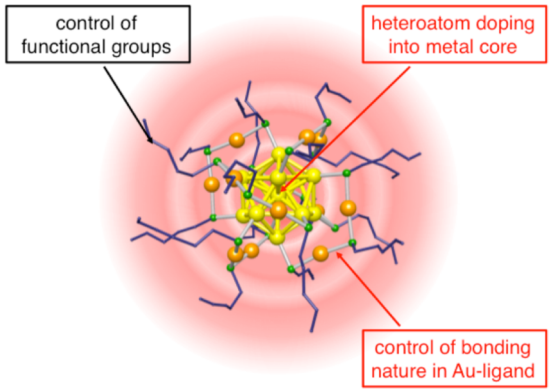

Figure 2. Effective methods for controlling the physical and chemical properties of magic $Au_n(SR)_m$ clusters.

the solubility of a cluster in a solvent, the interaction between a cluster and another material, the photoluminescence properties,[38,39] the optical activity,[40] and the redox behavior[41] of magic $Au_n(SR)_m$ clusters have been controlled by selecting appropriate functional groups. Moreover, new properties, such as responsiveness to an external stimulus[42] and molecular recognition capability,[43] have also been imparted to magic $Au_n(SR)_m$ clusters by the introduction of functional ligands to the clusters. In recent years, methods to synthesize the clusters while controlling the number of introduced ligands have also been established.[44−46] Through this type of research,[47] a great deal of knowledge has been gained relating to imparting functions to magic $Au_n(SR)_m$ clusters.

In addition to the method described above, heteroatom doping is also expected to become an effective method for imparting new physical and chemical properties to magic $Au_n(SR)_m$ clusters (Figure 2). Numerous gas-phase clusters[48] and metal nanoparticles[49−51] have been reported where heteroatom doping has led to changes in the physical and chemical properties of the clusters. This is also expected for magic $Au_n(SR)_m$ clusters. Therefore, clarification of the heteroatom doping effect on magic $Au_n(SR)_m$ clusters is expected to lead to the establishment of new functionalization methods for clusters.

Changing the nature of the bonding interactions between a metal and a ligand could also become an effective method for introducing new properties to clusters (Figure 2). Investigation of two-dimensional self-assembled monolayers (SAMs) revealed a decrease in the charge transfer from Au to the ligand in Au−selenolate (SeR) compared with that for Au−SR. It was also found that changing the nature of the bonding interaction in this way resulted in a stronger Au−SeR bond compared with the Au−SR bond,[52,53] as well as higher conductivity in the Au−SeR bond than that in the Au−SR bond.[54,55] This type of change in the bonding nature and the resulting changes in the physical and chemical properties are expected to occur even in clusters. Therefore, investigation of the physical and chemical properties of clusters protected by other chalcogenates (selenolates or tellurolates) is expected to lead to new functionalization methods for clusters.

Research into heteroatom doping and other chalcogenate protection has rapidly progressed in recent years. As a result, it has become clear that both heteroatom doping and other chalcogenate protection actually change the physical and chemical properties of magic $Au_n(SR)_m$ clusters. In this Perspective, we focus on studies relating to the three representative magic clusters $Au_{25}(SR)_{18}$, $Au_{38}(SR)_{24}$, and $Au_{144}(SR)_{60}$, discuss the knowledge gained thus far, and address future issues.

Heteroatom Doping. The first report of heteroatom doping of magic $Au_n(SR)_m$ clusters was in 2009 by Murray et al.[56] for the synthesis of $Au_{24}Pd(SR)_{18}$. Following on from this work, numerous reports on heteroatom doping have been published for $Au_{25}(SR)_{18}$, $Au_{38}(SR)_{24}$, and $Au_{144}(SR)_{60}$.

Pd, Pt, Ag, and Cu have been reported as doping elements. In most reports, the heteroatom-doped clusters were prepared by adding a reducing agent to a solution containing a gold salt, a metallic salt of the doping element, and a thiol (e.g., $C_{12}H_{25}SH$ or PhC_2H_4SH). For this type of synthetic method, where two different elements are simultaneously reduced, the almost simultaneous reduction of the doping element with gold via a reducing agent is necessary to form the doped cluster. Based on the redox potentials of the precursor metal ions, one would expect Pd, Pt, Ag, and Cu to be almost simultaneously reduced with Au by a reducing agent. This behavior is presumed to be related to the successful doping of Pd, Pt, Ag, and Cu into magic $Au_n(SR)_m$ clusters.

For clusters synthesized in this way, a significant amount of information has been obtained regarding the doping position. For $Au_{24}Pd(SR)_{18}$, after theoretical prediction by Häkkinen et al.,[57] our group[58] and Tsukuda et al.[59] experimentally verified the formation of a core−shell-type $Pd@Au_{24}(SR)_{18}$ structure (Figure 3a), in which the central Au atom in $Au_{25}(SR)_{18}$ (Figure 1) is replaced by Pd. On the basis of the experimental results, we also predicted that $Au_{36}Pd_2(SC_2H_4Ph)_{24}$ would have a similar core−shell-type structure (Figure 3b).[60] The larger $Au_{144}(SC_2H_4Ph)_{60}$ cluster was doped with up to seven Pd atoms, and Dass et al.[61] proposed that $Au_{144-n}Pd_n(SC_2H_4Ph)_{60}$ (n = 1−7) (Figure 3c) also had a core−shell-type metal core, with Pd as the core and Au as the shell. Jin et al.[62] and Zhang et al.[63] proposed that the doping of $Au_{25}(SC_2H_4Ph)_{18}$ with Pt, which belongs to the same group as Pd in the periodic table, afforded a core−shell-type $Pt@Au_{24}(SC_2H_4Ph)_{18}$ structure (Figure 3d) that was similar to that of $Au_{24}Pd(SR)_{18}$. Thus, both Pd and Pt are considered to be doped into the central position of the metal core regardless of the cluster size. Pd (131 meV $Å^{-2}$)[50] and Pt (159 meV $Å^{-2}$)[50] have larger surface energies than Au (96.8 meV $Å^{-2}$).[50] It is considered that this is one of the reasons why these elements are doped in the central position of the metal core rather than on the surface of the metal core.[61]

Interestingly, Ag is doped at a different position to Pd in thiolate-protected gold clusters. Walter et al.[64] predicted that Ag would be doped onto the surface of the metal core based on

dx.doi.org/10.1021/jz501941p | J. Phys. Chem. Lett. 2014, 5, 4134−4142

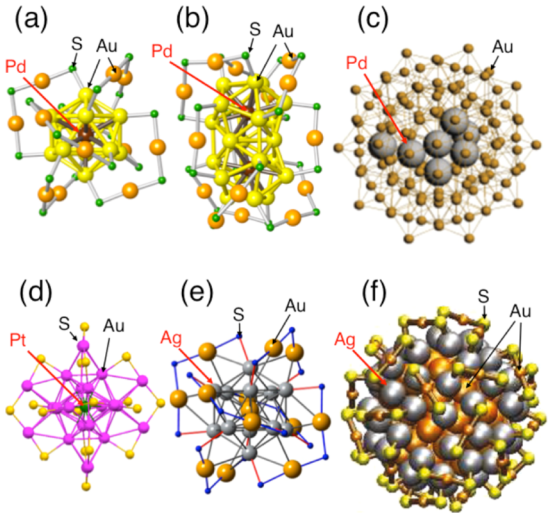

Figure 3. Geometrical structures determined or proposed for (a) $Au_{24}Pd(SR)_{18}$ (refs 57−59), (b) $Au_{36}Pd_2(SR)_{24}$ (ref 60), (c) $Au_{137}Pd_7(SR)_{60}$ (ref 61), (d) $Au_{24}Pt(SR)_{18}$ (refs 62 and 63), (e) $Au_{25-n}Ag_n(SR)_{18}$ (ref 70), and (f) $Au_{84}Ag_{60}(SR)_{60}$ (ref 73). The R groups have been omitted for clarity in all of the figure parts, and S is also omitted in (c). The figures were adapted from refs 58, 60−62 70, and 73. (Reference 61 was reproduced with permission of The Royal Society of Chemistry.)

density functional theory (DFT) calculations of $Au_{24}Ag(SCH_3)_{18}$. We investigated $Au_{25-n}Ag_n(SC_{12}H_{25})_{18}$ (n = 1−11) doped with up to 11 Ag atoms experimentally, and the results suggested that all of the Ag atoms were doped onto the surface of the metal core.[65] Aikens et al.[66] and Kauffman et al.[67] reached a similar conclusion using DFT calculations, and Xie et al.[68] and Yao et al.[69] obtained similar results by experimental studies. Very recently, Dass et al. verified that $Au_{25-n}Ag_n(SC_2H_4Ph)_{18}$ (n = 4−8) does indeed possess the predicted structure (Figure 3e) by single-crystal X-ray structural analysis.[70] Dass et al.[71,72] also successfully synthesized $Au_{38-n}Ag_n(SC_2H_4Ph)_{24}$ (n = 1−12) and $Au_{144-n}Ag_n(SC_2H_4Ph)_{60}$ (n = 1−60) and concluded that the majority of the Ag atoms were positioned on the surface of the metal core of these clusters. Häkkinen et al.[73] reached a similar conclusion for $Au_{144-n}Ag_n(SH_3)_{60}$ using DFT calculations (Figure 3f). On the basis of the results of these studies, Ag can be considered to be doped onto the surface of the metal core. Ag has a lower surface energy (78.0 meV Å^{-2}) than Au (96.8 meV Å^{-2}).[50] Therefore, Ag doping on the surface of thiolate-protected clusters would increase the stability of the clusters.

Information about Cu doping is scarce, and a clear understanding of the preferred doping position has not yet been established. Cu has a higher surface energy (113.9 meV Å^{-2}) than Au (96.8 meV Å^{-2}).[50] Moreover, Cu has a smaller atomic radius (1.28 Å) than Au (1.44 Å).[50] On the basis of these points, we initially concluded that Cu is located at the center of the metal core in $Au_{24}Cu(SR)_{18}$.[74] However, the optical absorption spectrum of $Cu@Au_{24}(SCH_3)_{18}$ obtained by DFT calculations did not agree well with the measured absorption spectrum for $Au_{\sim24}Cu_{\sim1}(SR)_{18}$.[74] Cu doping has also been achieved for $Au_{144-n}Cu_n(SR)_{60}$ (n = 1−23) clusters by Dass et al.[75] However, further research relating to the geometric structures of these clusters is necessary to provide a better understanding of the doping position in these clusters.

Several groups have attempted to determine whether doping of heteroatoms into magic $Au_n(SR)_m$ clusters leads to significant changes in the physical and chemical properties of the cluster. It was found that doping of Pd or Pt into $Au_{25}(SR)_{18}$ resulted in an increase of the stability of the cluster for decomposition in solution under severe conditions (high temperature[58] (Figure 4a) or in the presence of H_2O_2 (ref 62)).

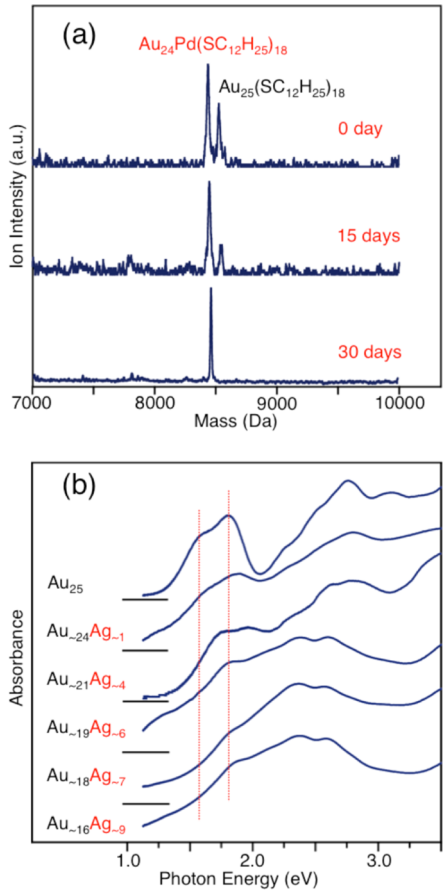

Figure 4. (a) Effect of Pd doping on the stability of $Au_{25}(SC_{12}H_{25})_{18}$ toward decomposition in a toluene solution at 50 °C. The stability was studied by measuring the time dependence of the mass spectrum of a mixture of $Au_{24}Pd(SC_{12}H_{25})_{18}$ and $Au_{25}(SC_{12}H_{25})_{18}$. (b) Effect of Ag doping on the electronic structure of $Au_{25}(SC_{12}H_{25})_{18}$, which was studied by measuring the optical absorption spectra of a series of $Au_{25-n}Ag_n(SC_{12}H_{25})_{18}$ toluene solutions. The characteristic peaks in the region of 1.5−2.0 eV of $Au_{25}(SC_{12}H_{25})_{18}$ are attributed to the highest occupied molecular orbital (HOMO) to lowest unoccupied molecular orbital (LUMO) transition based on DFT calculations of $Au_{25}(SCH_3)_{18}$.[12,13,17] Increased Ag doping shifts these peaks to higher energy, indicating an associated steady increase in the HOMO−LUMO gap of the cluster. The figure images were adapted from refs 58 (reproduced with permission of The Royal Society of Chemistry) and 65 (reproduced with permission of the PCCP Owner Societies).

Jiang et al.[76] predicted by DFT calculations that substitution of the central Au in $Au_{25}(SR)_{18}$ with Pd or Pt would lead to an increase in the interaction energy between the central atom and the surrounding cage structure. On the basis of their theoretical prediction, it is considered that a stronger metal core than $Au_{25}(SR)_{18}$ would be formed when the central atom was substituted with Pd or Pt, which would result in a highly stable cluster. In addition, $Au_{25}(SR)_{18}$ possesses an icosahedral metal core (Figure 1), where the spacing between the surface atoms

dx.doi.org/10.1021/jz501941p | J. Phys. Chem. Lett. 2014, 5, 4134−4142

must be about 5% greater than the interatomic spacing between the central atom and the surface atoms to allow encapsulation of the central atom. Substitution of the central Au atom (atomic radius = 1.44 Å)[50] in this cluster with Pd (i.d. = 1.38 Å)[50] or Pt (i.d. = 1.39 Å)[50] may resolve this type of geometric strain and result in an increase in the geometric stabilization of the cluster. Several other doping effects have also been reported for these elements. For example, we reported that the doping of $Au_{25}(SC_{12}H_{25})_{18}$ with Pd led to an improvement in the reactivity of this cluster with respect to the ligand exchange reaction.[77] Jin et al.[62,78] reported that doping $Au_{25}(SC_2H_4Ph)_{18}$ with Pt led to an improvement in the catalytic activity of the cluster for the oxidation of styrene, as well as a change of the HOMO−LUMO gap of the cluster. On the basis of these results, Pd and Pt doping can be considered to be effective methods to create more stable or more reactive clusters compared with the magic $Au_{25}(SR)_{18}$ cluster.

On the other hand, compared with Pd and Pt, more Ag and Cu can be doped in the $Au_n(SR)_m$ clusters. When the $Au_n(SR)_m$ clusters are doped with Ag or Cu, the physical and chemical properties of clusters can be continuously changed by controlling the number of the doped atoms.[65,66,79] For example, the doping of $Au_{25}(SR)_{18}$ with Ag led to a continuous increase in the HOMO−LUMO gap of the cluster as the number of dopant atoms increased (Figure 4b).[65,66,79] In addition, the emission wavelength of photoluminescence continuously shifted to a shorter wavelength as the number of dopants increased,[65] which might be related to the increase in the HOMO−LUMO gap of the cluster. Thus, Ag and Cu doping are considered to be effective methods to continuously change the electronic structure of a cluster. This method could be used to finely control the HOMO−LUMO gap of the cluster.

Heteroatom doping has the potential to create unique clusters that are more functionally useful and stable than the corresponding magic $Au_n(SR)_m$ clusters. Therefore, heteroatom doping is a useful method to functionalize magic $Au_n(SR)_m$ clusters.

Thus, heteroatom doping changes the physical and chemical properties of the cluster. This method has the potential to create clusters that are more functionally useful and stable than magic $Au_n(SR)_m$ clusters. Hence, one can consider that heteroatom doping is a useful method for the functionalization of magic $Au_n(SR)_m$ clusters.

For this type of functionalization method, systematic research is expected to be performed in the future. At present, the available information is overly fragmented, and clear design guidelines for selecting elements to impart specific functions to clusters have not been determined. For example, it has been reported that doping with Pd or Pt is an effective method for improving stability.[58,62] However, a general consensus has not been reached regarding which of these two elements is the most appropriate for improving the stability of a cluster. It is expected that measurements of various physical and chemical properties will be conducted for the four doped clusters $Au_{24}Pd(SR)_{18}$, $Au_{24}Pt(SR)_{18}$, $Au_{25-n}Ag_n(SR)_{18}$, and $Au_{25-n}Cu_n(SR)_{18}$ under the same experimental conditions. This systematic research will provide clear design guidelines for selecting elements to impart specific functions to clusters. In addition, a new high-resolution separation method is expected to be established to separate clusters doped with Ag or Cu based on the quantity of added dopant atoms, which would lead to further understanding of the heteroatom doping effect.

Moreover, from the viewpoint of enhancing the "library" of methods, the establishment of doping method for elements other than Pd, Pt, Ag, and Cu (refs 76 and 80−82) is also required. As described above, most of the doped clusters have been synthesized by a method involving the simultaneous reduction of two different types of elements. However, it is assumed that it will not be possible to dope with elements that have a significantly different redox potential than gold by this method, even if the products are chemically stable. Although DFT calculations predicted that a more stable metal core than that of $Au_{25}(SR)_{18}$ could be formed by the replacement of the central atom with Ni,[76] we have not yet succeeded in the synthesis of $Ni@Au_{24}(SR)_{18}$ using the simultaneous reduction method, despite numerous experimental trials over a period of several years. It should be noted that clusters doped with Cr, Mn, and Fe, whose magnetic properties have been studied by DFT calculations,[80−82] have also not been synthesized by the simultaneous reduction method. The significant difference in the redox potentials of Au and these elements is presumed to be the main reason for the unsuccessful synthesis. Therefore, a method other than simultaneous reduction is probably required to achieve doping with new elements.[83] In a study using phosphine as the ligand, Fischer et al.[84] proposed a novel synthetic method based on an entirely different concept to the simultaneous reduction method, and they successfully synthesized a core−shell-type $Ni@Au_{12}$ cluster using their new method.[84] Reacting this type of $Ni@Au_{12}$ cluster with a thiol may be an effective method to synthesize $Ni@Au_{24}(SR)_{18}$.[85] Furthermore, to the best of our knowledge, there have been no reports concerning the synthesis of clusters doped with two or more different elements (i.e., tri- or tetra-metal clusters). However, this is considered to also be an effective strategy to enhance the library of functionalization methods.

Protection with Other Chalcogenates. In recent years, there have been several reports about $Au_{25}(SeR)_{18}$ and $Au_{38}(SeR)_{24}$, which contain SeR as the ligand. These $Au_n(SeR)_m$ clusters have been reported to possess similar framework structures to magic $Au_n(SR)_m$ clusters (Figure 5).[86−89] All the results of the optical absorption spectroscopy, X-ray absorption fine structure analysis, and DFT calculations for $Au_{25}(SeR)_{18}$ and $Au_{38}(SeR)_{24}$ (R = $C_{12}H_{25}$ or C_8H_{17}) strongly support this interpretation.[87,89] However, the geometric structures of $Au_{24}(SePh)_{20}$ (ref 90) and $Au_{24}(SCH_2Ph{-}^tBu)_{20}$ (ref 91)

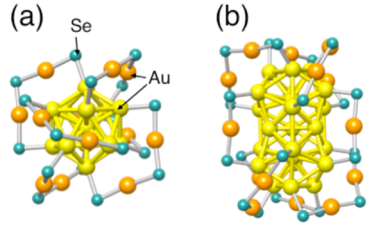

Figure 5. Geometrical structures proposed for (a) $Au_{25}(SeR)_{18}$ (refs 86−88) and (b) $Au_{38}(SeR)_{24}$ (ref 89). The R groups have been omitted for clarity. The figures were adapted from refs 87 and 89.

dx.doi.org/10.1021/jz501941p | J. Phys. Chem. Lett. 2014, 5, 4134−4142

determined by single-crystal X-ray structural analysis revealed that these two clusters possessed different geometric structures. For the $Au_n(SR)_m$ clusters, it has been revealed that when the ligand is changed from SC_2H_4Ph to SPh−^{t}Bu (thiolate with a phenyl group directly bonded to S), the same geometric structure cannot be maintained.[92,93] This type of effect is considered to have a significant role in the structural differences between $Au_{24}(SePh)_{20}$ and $Au_{24}(SCH_2Ph-^tBu)_{20}$. However, the possibility that the differences between Se and S also cause a change in the geometric structures of the clusters cannot be completely ruled out. Therefore, accurate determination of the geometric structures by single-crystal X-ray structural analysis is also required for $Au_{25}(SeR)_{18}$ and $Au_{38}(SeR)_{24}$.

Studies of synthesized clusters have revealed that changes in the bonding nature between Au and the ligand also occur in the cluster when the ligand is changed from SR to SeR. For example, in $Au_{25}(SeC_{12}H_{25})_{18}$, the nature of the charge transfer from Au to the ligand was reduced compared with that of $Au_{25}(SC_{12}H_{25})_{18}$ (Figure 6a).[86,89] A similar phenomenon has also been observed between $Au_{38}(SeC_{12}H_{25})_{24}$ and $Au_{38}(SC_{12}H_{25})_{24}$.[89] These results indicate that the covalent character of the bond between Au and the ligand increases when the ligand is changed from SR to SeR.

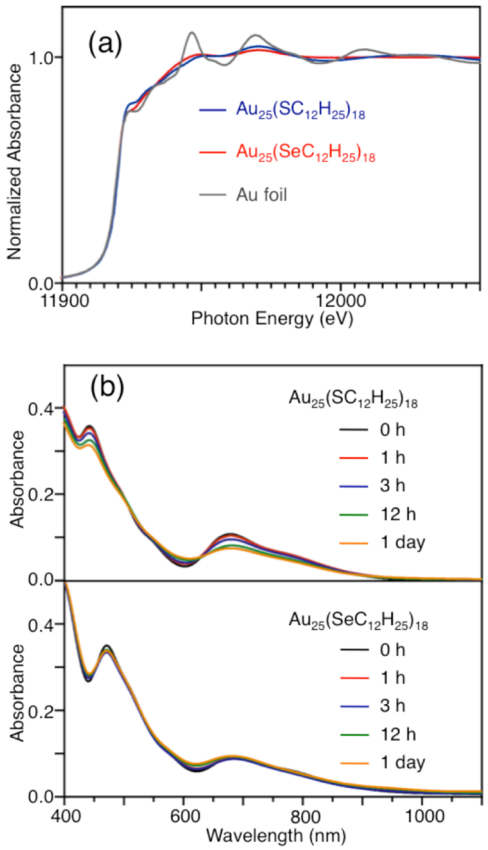

Figure 6. (a) Au L_3-edge XANES spectra of $Au_{25}(SC_{12}H_{25})_{18}$, $Au_{25}(SeC_{12}H_{25})_{18}$, and Au foil. For Au−S bonding, charge transfer from the Au 5d to the S 3d orbital takes place because of the difference in the electronegativities of the two elements. Therefore, the 5d electron density of $Au_n(SR)_m$ is lower than that of the Au foil, resulting in an increase in the white-line peak intensity, as seen for $Au_{25}(SC_{12}H_{25})_{18}$. The white-line peak intensity of $Au_{25}(SeC_{12}H_{25})_{18}$ is lower than that of $Au_{25}(SC_{12}H_{25})_{18}$, indicating that charge transfer is suppressed in Au−Se bonding compared with Au−S bonding. (b) Time dependence of the absorption spectra of $Au_{25}(SC_{12}H_{25})_{18}$ and $Au_{25}(SeC_{12}H_{25})_{18}$ toluene solutions at 60 °C. The figures were adapted from refs 87 and 89.

This change in the nature of the bonding changes the stability of the cluster with respect to decomposition in solution (Figure 6b). For example, when $Au_{25}(SR)_{18}$ (R = $C_{12}H_{25}$ or C_8H_{17}) is left in a solution under harsh conditions, it gradually dissociates (Figure 6b).[87] On the other hand, $Au_{25}(SeR)_{18}$ (R = $C_{12}H_{25}$ or C_8H_{17}) did not show any discernible decomposition when it was subjected to the same conditions for the same time (Figure 6b).[87] A similar result was also reported by Zhu et al.[88] These results indicate that the stability of $Au_{25}(SeR)_{18}$ is higher than that of $Au_{25}(SR)_{18}$ with respect to decomposition in solution. This type of decomposition in solution mainly occurs through a reaction where a thiolate or gold−thiolate complex is released from the cluster.[94] It is considered that the stability with respect to decomposition in solution is improved using SeR as the ligand because, as in SAMs, the Au−Se bond is stronger than Au−S, suppressing the dissociation reaction. These results demonstrate that using a SeR ligand is an effective method to create clusters with higher stability in solution than the corresponding $Au_n(SR)_m$ clusters.

In addition to improving the stability in solution, it is also expected that the use of SeR-based ligands will lead to significant improvements in the conductivity between the Au core and the ligand.[54,95] This function is highly desirable for the creation of molecular electronic devices using this type of gold clusters. However, such an effect has not yet been demonstrated experimentally. It is anticipated that the effect of using a SeR ligand on the conductivity between the gold core and the ligand will be elucidated in the future by comparing the conductivity[96] of a precisely synthesized $Au_n(SeR)_m$ clusters and the corresponding $Au_n(SR)_m$ clusters. With the exception of research about the effect of using SeR ligands on the stability, there have been very few reports about the general effects of using SeR ligands. However, it is anticipated that the effects of SeR ligands on other physical and chemical properties will also be elucidated in the future.

Changing the ligand to other chalcogenates changes the bonding nature between the metal and the ligand and thereby changes the physical and chemical properties of the clusters. Therefore, this type of change could also be an effective method for introducing new properties to magic clusters.

Regarding the conductivity between the ligand and the Au core, an even more dramatic effect is expected if tellurolate is used as the ligand.[97] With this in mind, we successfully synthesized $Au_{25}(TePh)_n(SC_8H_{17})_{18-n}$ (n = 1−18) containing TePh in the ligand shell (Figure 7).[98] Tong et al. reported that the oxidation of the tellurolate ligand occurred in a similar way to that observed in SAMs when 2.7 nm diameter gold nanoparticles were used as the metal core,[55,99] which resulted in the synthesis of $Au_n(OTeR)_m$ nanoparticles.[100] On the other hand, TePh was not oxidized in the cluster that we synthesized (Figure 7), which indicated that the TePh ligand could not be

dx.doi.org/10.1021/jz501941p | J. Phys. Chem. Lett. 2014, 5, 4134−4142

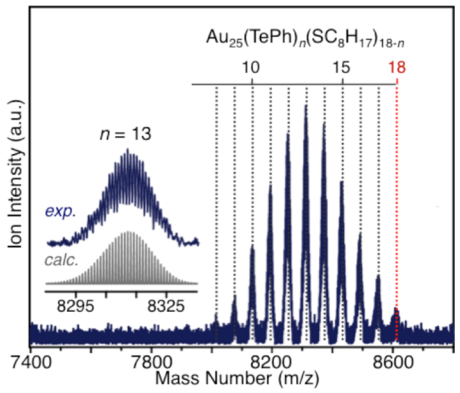

Figure 7. Negative-ion ESI mass spectrum of the products formed by the reaction between $Au_{25}(SC_8H_{17})_{18}$ and $(PhTe)_2$ with $[(PhTe)_2]/[Au_{25}(SC_8H_{17})_{18}] = 7.0$. The insets compare the experimental data with the calculated isotope pattern for the main peak in the mass spectrum. The figure was adapted from ref 98.

oxidized in this cluster. Thus, it is expected that the effect of tellurolate protection on the conductivity of the cluster can be clarified by comparing the conductivities of $Au_{25}(TePh)_{18}$ and $Au_{25}(SPh)_{18}$. It is expected that a method for the precise synthesis of $Au_{25}(TePh)_{18}$ will be established, and as a result, creation of stable clusters with high conductivity will be realized in the future.

Perspective. Establishing methods for the functionalization of magic $Au_n(SR)_m$ clusters would allow the conversion of magic $Au_n(SR)_m$ clusters into more functional and useful nanomaterials. Recent research on heteroatom doping and the use of the other chalcogenate ligands strongly suggests that these will become techniques for the functionalization of magic $Au_n(SR)_m$ clusters. Interestingly, these two techniques are independent of one another, as well as being independent of functional group control. Therefore, control of the functional groups, heteroatom doping, and control of the bonding nature could be used in combination. It is expected that a significant amount of information will be obtained about these three strategies in the future, and as a result, the library of functionalization methods will be expanded. If this can be achieved, stable nanomaterials with desired functions for specific applications could be synthesized by applying those methods to magic $Au_n(SR)_m$ clusters.

AUTHOR INFORMATION

Corresponding Author

*E-mail: negishi@rs.kagu.tus.ac.jp.

Notes

The authors declare no competing financial interest.

Biographies

Wataru Kurashige is an Assistant Professor in the Negishi group at Tokyo University of Science. He obtained his B.Sc. (2010), M.Sc. (2012), and Ph.D. (2014) in chemistry from Tokyo University of Science. His research interests include the functionalization of noble metal nanoclusters.

Yoshiki Niihori is a postdoctoral researcher in the Negishi group at Tokyo University of Science. He obtained his B.Sc. (2009), M.Sc. (2011), and Ph.D. (2014) in chemistry from Tokyo University of Science. His research interests include the development of high-resolution separation method for noble metal nanoclusters.

Sachil Sharma is a postdoctoral researcher in the Negishi group at Tokyo University of Science. He obtained his B.Sc. (1999) from Himachal Pradesh University, M.Sc. (2002) in chemistry from Maharshi Dayanand University, and Ph.D. (2011) in chemistry from the Indian Institute of Technology Kanpur. His research interests include the synthesis of the novel metal clusters.

Yuichi Negishi is an Associate Professor of Chemistry at Tokyo University of Science. He received his Ph.D. in chemistry in 2001 under the supervision of Prof. Atsushi Nakajima from Keio University. Before joining Tokyo University of Science in 2008, he was employed at Keio University and at the Institute for Molecular Science (IMS). His current research interests include the creation of stable and functionalized metal nanoclusters and their application as photocatalysts. Website: http://www.rs.kagu.tus.ac.jp/negishi/negishienglish.html.

ACKNOWLEDGMENTS

We acknowledge financial support from Grants-in-Aid for Scientific Research (Nos. 25288009, 25102539, and 26620016), the Canon Foundation, and the Iketani Science and Technology Foundation.

REFERENCES

(1) Brust, M.; Walker, M.; Bethell, D.; Schiffrin, D. J.; Whyman, R. Synthesis of Thiol-Derivatized Gold Nanoparticles in a Two-Phase Liquid–Liquid System. *J. Chem. Soc., Chem. Commun.* **1994**, *7*, 801–802.

(2) Tsukuda, T. Toward an Atomic-Level Understanding of Size-Specific Properties of Protected and Stabilized Gold Clusters. *Bull. Chem. Soc. Jpn.* **2012**, *85*, 151–168.

(3) Qian, H.; Zhu, M.; Wu, Z.; Jin, R. Quantum Sized Gold Nanoclusters with Atomic Precision. *Acc. Chem. Res.* **2012**, *45*, 1470–1479.

(4) Parker, J. F.; Fields-Zinna, C. A.; Murray, R. W. The Story of a Monodisperse Gold Nanoparticle: $Au_{25}L_{18}$. *Acc. Chem. Res.* **2010**, *43*, 1289–1296.

(5) Bigioni, T. P.; Whetten, R. L.; Dag, Ö. Near-Infrared Luminescence from Small Gold Nanocrystals. *J. Phys. Chem. B* **2000**, *104*, 6983–6986.

(6) Miller, S. A.; Womick, J. M.; Parker, J. F.; Murray, R. W.; Moran, A. M. Femtosecond Relaxation Dynamics of $Au_{25}L_{18}^-$ Monolayer-Protected Clusters. *J. Phys. Chem. C* **2009**, *113*, 9440–9444.

(7) Ramakrishna, G.; Varnavski, O.; Kim, J.; Lee, D.; Goodson, T. Quantum-Sized Gold Clusters as Efficient Two-Photon Absorbers. *J. Am. Chem. Soc.* **2008**, *130*, 5032–5033.

(8) Li, G.; Jin, R. Atomically Precise Gold Nanoclusters as New Model Catalysts. *Acc. Chem. Res.* **2013**, *46*, 1749–1758.

(9) Negishi, Y.; Nobusada, K.; Tsukuda, T. Glutathione-Protected Gold Clusters Revisited: Bridging the Gap between Gold(I)-Thiolate Complexes and Thiolate-Protected Gold Nanocrystals. *J. Am. Chem. Soc.* **2005**, *127*, 5261–5270.

(10) Negishi, Y.; Chaki, N. K.; Shichibu, Y.; Whetten, R. L.; Tsukuda, T. Origin of Magic Stability of Thiolated Gold Clusters: A Case Study on $Au_{25}(SC_6H_{13})_{18}$. *J. Am. Chem. Soc.* **2007**, *129*, 11322–11323.

(11) Heaven, M. W.; Dass, A.; White, P. S.; Holt, K. M.; Murray, R. W. Crystal Structure of the Gold Nanoparticle $[N(C_8H_{17})_4][Au_{25}(SCH_2CH_2Ph)_{18}]$. *J. Am. Chem. Soc.* **2008**, *130*, 3754–3755.

(12) Zhu, M.; Aikens, C. M.; Hollander, F. J.; Schatz, G. C.; Jin, R. Correlating the Crystal Structure of a Thiol-Protected Au_{25} Cluster and Optical Properties. *J. Am. Chem. Soc.* **2008**, *130*, 5883–5885.

(13) Akola, J.; Walter, M.; Whetten, R. L.; Häkkinen, H.; Grönbeck, H. On the Structure of Thiolate-Protected Au_{25}. *J. Am. Chem. Soc.* **2008**, *130*, 3756–3757.

(14) Dass, A.; Stevenson, A.; Dubay, G. R.; Tracy, J. B.; Murray, R. W. Nanoparticle MALDI-TOF Mass Spectrometry without Fragmen-

tation: $Au_{25}(SCH_2CH_2Ph)_{18}$ and Mixed Monolayer $Au_{25}(SCH_2CH_2Ph)_{18-x}(L)_x$. *J. Am. Chem. Soc.* **2008**, *130*, 5940−5946.
(15) Luo, Z.; Nachammai, V.; Zhang, B.; Yan, N.; Leong, D. T.; Jiang, D.-e.; Xie, J. Toward Understanding the Growth Mechanism: Tracing All Stable Intermediate Species from Reduction of Au(I)−Thiolate Complexes to Evolution of Au_{25} Nanoclusters. *J. Am. Chem. Soc.* **2014**, *136*, 10577−10580.
(16) Liu, C.; Lin, S.; Pei, Y.; Zeng, X. C. Semiring Chemistry of $Au_{25}(SR)_{18}$: Fragmentation Pathway and Catalytic Active Site. *J. Am. Chem. Soc.* **2013**, *135*, 18067−18079.
(17) Jiang, D.-e.; Kühn, M.; Tang, Q.; Weigend, F. Superatomic Orbitals under Spin−Orbit Coupling. *J. Phys. Chem. Lett.* **2014**, *5*, 3286−3289.
(18) Chaki, N. K.; Negishi, Y.; Tsunoyama, H.; Shichibu, Y.; Tsukuda, T. Ubiquitous 8 and 29 kDa Gold:Alkanethiolate Cluster Compounds: Mass Spectrometric Determination of Molecular Formulas and Structural Implications. *J. Am. Chem. Soc.* **2008**, *130*, 8608−8610.
(19) Qian, H.; Eckenhoff, W. T.; Zhu, Y.; Pintauer, T.; Jin, R. Total Structure Determination of Thiolate-Protected Au_{38} Nanoparticles. *J. Am. Chem. Soc.* **2010**, *132*, 8280−8281.
(20) Dolamic, I.; Knoppe, S.; Dass, A.; Bürgi, T. First Enantioseparation and Circular Dichroism Spectra of Au_{38} Clusters Protected by Achiral Ligands. *Nat. Commun.* **2012**, *3*, 798−803.
(21) Fields-Zinna, C. A.; Sardar, R.; Beasley, C. A.; Murray, R. W. Electrospray Ionization Mass Spectrometry of Intrinsically Cationized Nanoparticles, $[Au_{144/146}(SC_{11}H_{22}N(CH_2CH_3)_3^+)_x(S(CH_2)_5CH_3)_y]^{x+}$. *J. Am. Chem. Soc.* **2009**, *131*, 16266−16271.
(22) Malola, S.; Lehtovaara, L.; Enkovaara, J.; Häkkinen, H. Birth of the Localized Surface Plasmon Resonance in Monolayer-Protected Gold Nanoclusters. *ACS Nano* **2013**, *7*, 10263−10270.
(23) Bahena, D.; Bhattarai, N.; Santiago, U.; Tlahuice, A.; Ponce, A.; Bach, S. B. H.; Yoon, B.; Whetten, R. L.; Landman, U.; Jose-Yacaman, M. STEM Electron Diffraction and High-Resolution Images Used in the Determination of the Crystal Structure of the $Au_{144}(SR)_{60}$ Cluster. *J. Phys. Chem. Lett.* **2013**, *4*, 975−981.
(24) Weissker, H.-Ch; Escobar, H. B.; Thanthirige, V. D.; Kwak, K.; Lee, D.; Ramakrishna, G.; Whetten, R. L.; López-Lozano, X. Information on Quantum States Pervades the Visible Spectrum of the Ubiquitous $Au_{144}(SR)_{60}$ Gold Nanocluster. *Nat. Commun.* **2014**, *5*, 3785−3792.
(25) Walter, M.; Akola, J.; Lopez-Acevedo, O.; Jadzinsky, P. D.; Calero, G.; Ackerson, C. J.; Whetten, R. L.; Grönbeck, H.; Häkkinen, H. A Unified View of Ligand-Protected Gold Clusters as Superatom Complexes. *Proc. Natl. Acad. Sci. U.S.A* **2008**, *105*, 9157−9162.
(26) Cheng, L.; Ren, C.; Zhang, X.; Yang, J. New Insight into the Electronic Shell of $Au_{38}(SR)_{24}$: A Superatomic Molecule. *Nanoscale* **2013**, *5*, 1475−1478.
(27) Kauffman, D. R.; Alfonso, D.; Matranga, C.; Qian, H.; Jin, R. Experimental and Computational Investigation of Au_{25} Clusters and CO_2: A Unique Interaction and Enhanced Electrocatalytic Activity. *J. Am. Chem. Soc.* **2012**, *134*, 10237−10243.
(28) Wu, Z.; Jiang, D.-e.; Mann, A. K. P.; Mullins, D. R.; Qiao, Z.-A.; Allard, L. F.; Zeng, C.; Jin, R.; Overbury, S. H. Thiolate Ligands as a Double-Edged Sword for CO Oxidation on CeO_2 Supported $Au_{25}(SCH_2CH_2Ph)_{18}$ Nanoclusters. *J. Am. Chem. Soc.* **2014**, *136*, 6111−6122.
(29) Huang, P.; Chen, G.; Jiang, Z.; Jin, R.; Zhu, Y.; Sun, Y. Atomically Precise Au_{25} Superatoms Immobilized on CeO_2 Nanorods for Styrene Oxidation. *Nanoscale* **2013**, *5*, 3668−3672.
(30) Nie, X.; Zeng, C.; Ma, X.; Qian, H.; Ge, Q.; Xu, H.; Jin, R. CeO_2-Supported $Au_{38}(SR)_{24}$ Nanocluster Catalysts for CO Oxidation: A Comparison of Ligand-On and -Off Catalysts. *Nanoscale* **2013**, *5*, 5912−5918.
(31) Stamplecoskie, K. G.; Kamat, P. V. Size-Dependent Excited State Behavior of Glutathione-Capped Gold Clusters and Their Light-Harvesting Capacity. *J. Am. Chem. Soc.* **2014**, *136*, 11093−11099.
(32) Yu, C.; Li, G.; Kumar, S.; Kawasaki, H.; Jin, R. Stable $Au_{25}(SR)_{18}/TiO_2$ Composite Nanostructure with Enhanced Visible Light Photocatalytic Activity. *J. Phys. Chem. Lett.* **2013**, *4*, 2847−2852.
(33) Sakai, N.; Tatsuma, T. Photovoltaic Properties of Glutathione-Protected Gold Clusters Adsorbed on TiO_2 Electrodes. *Adv. Mater.* **2010**, *22*, 3185−3188.
(34) Nakata, K.; Sugawara, S.; Kurashige, W.; Negishi, Y.; Nagata, M.; Uchida, S.; Terashima, C.; Kondo, T.; Yuasa, M.; Fujishima, A. Cosensitization Properties of Glutathione-Protected Au_{25} Cluster on Ruthenium Dye-Sensitized TiO_2 Photoelectrode. *Int. J. Photoenergy* **2013**, *2013*, 456583.
(35) Chen, W.; Chen, S. Oxygen Electroreduction Catalyzed by Gold Nanoclusters: Strong Core Size Effects. *Angew. Chem., Int. Ed.* **2009**, *48*, 4386−4389.
(36) Kwak, K.; Kumar, S. S.; Pyo, K.; Lee, D. Ionic Liquid of a Gold Nanocluster: A Versatile Matrix for Electrochemical Biosensors. *ACS Nano* **2014**, *8*, 671−679.
(37) Kawasaki, H.; Kumar, S.; Li, G.; Zeng, C.; Kauffman, D. R.; Yoshimoto, J.; Iwasaki, Y.; Jin, R. Generation of Singlet Oxygen by Photoexcited $Au_{25}(SR)_{18}$ Clusters. *Chem. Mater.* **2014**, *26*, 2777−2788.
(38) Shibu, E. S.; Muhammed, M. A. H.; Tsukuda, T.; Pradeep, T. Ligand Exchange of $Au_{25}SG_{18}$ Leading to Functionalized Gold Clusters: Spectroscopy, Kinetics, and Luminescence. *J. Phys. Chem. C* **2008**, *112*, 12168−12176.
(39) Wu, Z.; Jin, R. On the Ligand's Role in the Fluorescence of Gold Nanoclusters. *Nano Lett.* **2010**, *10*, 2568−2573.
(40) Knoppe, S.; Bürgi, T. Chirality in Thiolate-Protected Gold Clusters. *Acc. Chem. Res.* **2014**, *47*, 1318−1326.
(41) Holm, A. H.; Ceccato, M.; Donkers, R. L.; Fabris, L.; Pace, G.; Maran, F. Effect of Peptide Ligand Dipole Moments on the Redox Potentials of Au_{38} and Au_{140} Nanoparticles. *Langmuir* **2006**, *22*, 10584−10589.
(42) Negishi, Y.; Kurashige, W.; Niihori, Y.; Nobusada, K. Toward the Creation of Stable, Functionalized Metal Clusters. *Phys. Chem. Chem. Phys.* **2013**, *15*, 18736−18751.
(43) Hassinen, J.; Pulkkinen, P.; Kalenius, E.; Pradeep, T.; Tenhu, H.; Häkkinen, H.; Ras, R. H. A. Mixed-Monolayer-Protected Au_{25} Clusters with Bulky Calix[4]arene Functionalities. *J. Phys. Chem. Lett.* **2014**, *5*, 585−589.
(44) Niihori, Y.; Matsuzaki, M.; Pradeep, T.; Negishi, Y. Separation of Precise Compositions of Noble Metal Clusters Protected with Mixed Ligands. *J. Am. Chem. Soc.* **2013**, *135*, 4946−4949.
(45) Yuan, X.; Zhang, B.; Luo, Z.; Yao, Q.; Leong, D. T.; Yan, N.; Xie, J. Balancing the Rate of Cluster Growth and Etching for Gram-Scale Synthesis of Thiolate-Protected Au_{25} Nanoclusters with Atomic Precision. *Angew. Chem., Int. Ed.* **2014**, *53*, 4623−4627.
(46) Niihori, Y.; Matsuzaki, M.; Uchida, C.; Negishi, Y. Advanced Use of High-Performance Liquid Chromatography for Synthesis of Controlled Metal Clusters. *Nanoscale* **2014**, *6*, 7889−7896.
(47) Ni, T. W.; Tofanelli, M. A.; Phillips, B. D.; Ackerson, C. J. Structural Basis for Ligand Exchange on $Au_{25}(SR)_{18}$. *Inorg. Chem.* **2014**, *53*, 6500−6502.
(48) Akutsu, M.; Koyasu, K.; Atobe, J.; Hosoya, N.; Miyajima, K.; Mitsui, M.; Nakajima, A. Experimental and Theoretical Characterization of Aluminum-Based Binary Superatoms of $Al_{12}X$ and Their Cluster Salts. *J. Phys. Chem. A* **2006**, *110*, 12073−12076.
(49) Sanker, M.; Dimitratos, N.; Miedziak, P. J.; Wells, P. P.; Kiely, C. J.; Hutchings, G. J. Designing Bimetallic Catalysts for a Green and Sustainable Future. *Chem. Soc. Rev.* **2012**, *41*, 8099−8139.
(50) Ferrando, R.; Jellinek, J.; Johnston, R. L. Nanoalloys: From Theory to Applications of Alloy Clusters and Nanoparticles. *Chem. Rev.* **2008**, *108*, 845−910.
(51) Zhang, H.; Watanabe, T.; Okumura, M.; Haruta, M.; Toshima, N. Catalytically Highly Active Top Gold Atom on Palladium Nanocluster. *Nat. Mater.* **2012**, *11*, 49−52.
(52) de la Llave, E.; Scherlis, D. A. Selenium-Based Self Assembled Monolayers: The Nature of Adsorbate−Surface Interactions. *Langmuir* **2010**, *26*, 173−178.

(53) Szelagowska-Kunstman, K.; Cyganik, P.; Schüpbach, B.; Terfort, A. Relative Stability of Thiol and Selenol Based SAMs on Au(111) — Exchange Experiments. *Phys. Chem. Chem. Phys.* **2010**, *12*, 4400−4406.
(54) Romashov, L. V.; Ananikov, V. P. Self-Assembled Selenium Monolayers: From Nanotechnology to Materials Science and Adaptive Catalysis. *Chem.—Eur. J.* **2013**, *19*, 17640−17660.
(55) Yokota, K.; Taniguchi, M.; Kawai, T. Control of the Electrode−Molecule Interface for Molecular Devices. *J. Am. Chem. Soc.* **2007**, *129*, 5818−5819.
(56) Fields-Zinna, C. A.; Crowe, M. C.; Dass, A.; Weaver, J. E. F.; Murray, R. W. Mass Spectrometry of Small Bimetal Monolayer-Protected Clusters. *Langmuir* **2009**, *25*, 7704−7710.
(57) Kacprzak, K. A.; Lehtovaara, L.; Akola, J.; Lopez-Acevedo, O.; Häkkinen, H. A Density Functional Investigation of Thiolate-Protected Bimetal $PdAu_{24}(SR)_{18}^{z}$ Clusters: Doping the Superatom Complex. *Phys. Chem. Chem. Phys.* **2009**, *11*, 7123−7129.
(58) Negishi, Y.; Kurashige, W.; Niihori, Y.; Iwasa, T.; Nobusada, K. Isolation, Structure, and Stability of a Dodecanethiolate-Protected Pd_1Au_{24} Cluster. *Phys. Chem. Chem. Phys.* **2010**, *12*, 6219−6225.
(59) Negishi, Y.; Kurashige, K.; Kobayashi, Y.; Yamazoe, Y.; Kojima, N.; Seto, M.; Tsukuda, T. Formation of a Pd@Au_{12} Superatomic Core in $Au_{24}Pd_1(SC_{12}H_{25})_{18}$ Probed by ^{197}Au Mössbauer and Pd K-Edge EXAFS Spectroscopy. *J. Phys. Chem. Lett.* **2013**, *4*, 3579−3583.
(60) Negishi, Y.; Igarashi, K.; Munakata, K.; Ohgake, W.; Nobusada, K. Palladium Doping of Magic Gold Cluster $Au_{38}(SC_2H_4Ph)_{24}$: Formation of $Pd_2Au_{36}(SC_2H_4Ph)_{24}$ with Higher Stability than $Au_{38}(SC_2H_4Ph)_{24}$. *Chem. Commun.* **2012**, *48*, 660−662.
(61) Kothalawala, N.; Kumara, C.; Ferrando, R.; Dass, A. $Au_{144-x}Pd_x(SR)_{60}$ Nanomolecules. *Chem. Commun.* **2013**, *49*, 10850−10852.
(62) Qian, H.; Jiang, D.-e.; Li, G.; Gayathri, C.; Das, A.; Gil, R. R.; Jin, R. Monoplatinum Doping of Gold Nanoclusters and Catalytic Application. *J. Am. Chem. Soc.* **2012**, *134*, 16159−16162.
(63) Christensen, S. L.; MacDonald, M. A.; Chatt, A.; Zhang, P.; Qian, H.; Jin, R. Dopant Location, Local Structure, and Electronic Properties of $Au_{24}Pt(SR)_{18}$ Nanoclusters. *J. Phys. Chem. C* **2012**, *116*, 26932−26937.
(64) Walter, M.; Moseler, M. Ligand-Protected Gold Alloy Clusters: Doping the Superatom. *J. Phys. Chem. C* **2009**, *113*, 15834−15837.
(65) Negishi, Y.; Iwai, T.; Ide, M. Continuous Modulation of Electronic Structure of Stable Thiolate-Protected Au_{25} Cluster by Ag Doping. *Chem. Commun.* **2010**, *46*, 4713−4715.
(66) Guidez, E. B.; Mäkinen, V.; Häkkinen, H.; Aikens, C. M. Effects of Silver Doping on the Geometric and Electronic Structure and Optical Absorption Spectra of the $Au_{25-n}Ag_n(SH)_{18}^{-}$ (n = 1, 2, 4, 6, 8, 10, 12) Bimetallic Nanoclusters. *J. Phys. Chem. C* **2012**, *116*, 20617−20624.
(67) Kauffman, D. R.; Alfonso, D.; Matranga, C.; Qian, H.; Jin, R. A Quantum Alloy: The Ligand-Protected $Au_{25-n}Ag_n(SR)_{18}$ Cluster. *J. Phys. Chem. C* **2013**, *117*, 7914−7923.
(68) Dou, X.; Yuan, X.; Yao, Q.; Luo, Z.; Zheng, K.; Xie, J. Facile Synthesis of Water-Soluble $Au_{25-x}Ag_x$ Nanoclusters Protected by Mono- and Bi-thiolate Ligands. *Chem. Commun.* **2014**, *50*, 7459−7462.
(69) Kobayashi, R.; Nonoguchi, Y.; Sasaki, A.; Yao, H. Chiral Monolayer-Protected Bimetallic Au−Ag Nanoclusters: Alloying Effect on Their Electronic Structure and Chiroptical Activity. *J. Phys. Chem. C* **2014**, *118*, 15506−15515.
(70) Kumara, C.; Aikens, C. M.; Dass, A. X-ray Crystal Structure and Theoretical Analysis of $Au_{25-x}Ag_x(SCH_2CH_2Ph)_{18}^{-}$ Alloy. *J. Phys. Chem. Lett.* **2014**, *5*, 461−466.
(71) Kumara, C.; Dass, A. AuAg Alloy Nanomolecules with 38 Metal Atoms. *Nanoscale* **2012**, *4*, 4084−4086.
(72) Kumara, C.; Dass, A. $(AuAg)_{144}(SR)_{60}$ Alloy Nanomolecules. *Nanoscale* **2011**, *3*, 3064−3067.
(73) Malola, S.; Häkkinen, H. Electronic Structure and Bonding of Icosahedral Core−Shell Gold−Silver Nanoalloy Clusters $Au_{144-x}Ag_x(SR)_{60}$. *J. Phys. Chem. Lett.* **2011**, *2*, 2316−2321.
(74) Negishi, Y.; Munakata, K.; Ohgake, W.; Nobusada, K. Effect of Copper Doping on Electronic Structure, Geometric Structure, and Stability of Thiolate-Protected Au_{25} Nanoclusters. *J. Phys. Chem. Lett.* **2012**, *3*, 2209−2214.
(75) Dharmaratne, A. C.; Dass, A. $Au_{144-x}Cu_x(SC_6H_{13})_{60}$ Nanomolecules: Effect of Cu Incorporation on Composition and Plasmon-Like Peak Emergence in Optical Spectra. *Chem. Commun.* **2014**, *50*, 1722−1724.
(76) Jiang, D.-e.; Dai, S. From Superatomic $Au_{25}(SR)_{18}^{-}$ to Superatomic M@$Au_{24}(SR)_{18}^{q}$ Core−Shell Clusters. *Inorg. Chem.* **2009**, *48*, 2720−2722.
(77) Niihori, Y.; Kurashige, W.; Matsuzaki, M.; Negishi, Y. Remarkable Enhancement in Ligand-Exchange Reactivity of Thiolate-Protected Au_{25} Nanoclusters by Single Pd Atom Doping. *Nanoscale* **2013**, *5*, 508−512.
(78) Jin, R.; Nobusada, K. Doping and Alloying in Atomically Precise Gold Nanoparticles. *Nano Res.* **2014**, *7*, 285−300.
(79) Tlahuice, A.-F. Optical Properties of Thiolate-Protected $Ag_nAu_{25-n}(SCH_3)_{18}^{-}$ Clusters. *J. Nanopart. Res.* **2013**, *15*, 1771.
(80) Jiang, D.-e.; Whetten, R. L. Magnetic Doping of a Thiolated-Gold Superatom: First-Principles Density Functional Theory Calculations. *Phys. Rev. B* **2009**, *80*, 115402.
(81) Reveles, J. U.; Clayborne, P. A.; Reber, A. C.; Khanna, S. N.; Pradhan, K.; Sen, P.; Pederson, M. R. Designer Magnetic Superatoms. *Nat. Chem.* **2009**, *1*, 310−315.
(82) Zhou, M.; Cai, Y. Q.; Zeng, M. G.; Zhang, C.; Feng, Y. P. Mn-Doped Thiolated Au_{25} Nanoclusters: Atomic Configuration, Magnetic Properties, and a Possible High-Performance Spin Filter. *Appl. Phys. Lett.* **2011**, *98*, 143103.
(83) Wu, Z. Anti-Galvanic Reduction of Thiolate-Protected Gold and Silver Nanoparticles. *Angew. Chem., Int. Ed.* **2012**, *51*, 2934−2938.
(84) Puls, A.; Jerabek, P.; Kurashige, W.; Förster, M.; Molon, M.; Bollermann, T.; Winter, M.; Gemel, C.; Negishi, Y.; Frenking, G.; Fischer, R. A. A Novel Concept for the Synthesis of Multiply Doped Gold Clusters $[(M@Au_nM'_m)L_k]^{q+}$. *Angew. Chem., Int. Ed.* **2014**, *53*, 4327−4331.
(85) Shichibu, Y.; Negishi, Y.; Tsukuda, T.; Teranishi, T. Large-Scale Synthesis of Thiolated Au_{25} Clusters via Ligand Exchange Reactions of Phosphine-Stabilized Au_{11} Clusters. *J. Am. Chem. Soc.* **2005**, *127*, 13464−13465.
(86) Negishi, Y.; Kurashige, W.; Kamimura, U. Isolation and Structural Characterization of an Octaneselenolate-Protected Au_{25} Cluster. *Langmuir* **2011**, *27*, 12289−12292.
(87) Kurashige, W.; Yamaguchi, M.; Nobusada, K.; Negishi, Y. Ligand-Induced Stability of Gold Nanoclusters: Thiolate versus Selenolate. *J. Phys. Chem. Lett.* **2012**, *3*, 2649−2652.
(88) Meng, X.; Xu, Q.; Wang, S.; Zhu, M. Ligand-Exchange Synthesis of Selenophenolate-Capped Au_{25} Nanoclusters. *Nanoscale* **2012**, *4*, 4161−4165.
(89) Kurashige, W.; Yamazoe, S.; Kanehira, K.; Tsukuda, T.; Negishi, Y. Selenolate-Protected Au_{38} Nanoclusters: Isolation and Structural Characterization. *J. Phys. Chem. Lett.* **2013**, *4*, 3181−3185.
(90) Song, Y.; Wang, S.; Zhang, J.; Kang, X.; Chen, S.; Li, P.; Sheng, H.; Zhu, M. Crystal Structure of Selenolate-Protected $Au_{24}(SeR)_{20}$ Nanocluster. *J. Am. Chem. Soc.* **2014**, *136*, 2963−2965.
(91) Das, A.; Li, T.; Li, G.; Nobusada, K.; Zeng, C.; Rosi, N. L.; Jin, R. Crystal Structure and Electronic Properties of a Thiolate-Protected Au_{24} Nanocluster. *Nanoscale* **2014**, *6*, 6458−6462.
(92) Zeng, C.; Qian, H.; Li, T.; Li, G.; Rosi, N. L.; Yoon, B.; Barnett, R. N.; Whetten, R. L.; Landman, U.; Jin, R. Total Structure and Electronic Properties of the Gold Nanocrystal $Au_{36}(SR)_{24}$. *Angew. Chem., Int. Ed.* **2012**, *124*, 13291−13295.
(93) Zeng, C.; Liu, C.; Pei, Y.; Jin, R. Thiol Ligand-Induced Transformation of $Au_{38}(SC_2H_4Ph)_{24}$ to $Au_{36}(SPh\text{-}t\text{-}Bu)_{24}$. *ACS Nano* **2013**, *7*, 6138−6145.
(94) Shichibu, Y.; Negishi, Y.; Tsunoyama, H.; Kanehara, M.; Teranishi, T.; Tsukuda, T. Extremely High Stability of Glutathionate-Protected Au_{25} Clusters Against Core Etching. *Small* **2007**, *3*, 835−839.
(95) Li, Y.; Zaluzhna, O.; Xu, B.; Gao, Y.; Modest, J. M.; Tong, Y. Y. J. Mechanistic Insight into the Brust−Schiffrin Two-Phase Synthesis of

Organo-chalcogenate-Protected Metal Nanoparticles. *J. Am. Chem. Soc.* **2011**, *133*, 2092−2095.
(96) Kano, S.; Azuma, Y.; Kanehara, M.; Teranishi, T.; Majima, Y. Room-Temperature Coulomb Blockade from Chemically Synthesized Au Nanoparticles Stabilized by Acid−Base Interaction. *Appl. Phys. Express* **2010**, *3*, 105003.
(97) Li, Y.; Love, O.; Tong, Y. Y. J. Small Gold Nanoparticles Synthesized with Dialkyl Ditelluride. *Nano Bull.* **2013**, *2*, 130221.
(98) Kurashige, W.; Yamazoe, S.; Yamaguchi, M.; Nishido, K.; Nobusada, K.; Tsukuda, T.; Negishi, Y. Au_{25} Clusters Containing Unoxidized Tellurolates in the Ligand Shell. *J. Phys. Chem. Lett.* **2014**, *5*, 2072−2076.
(99) Nakamura, T.; Yasuda, S.; Miyamae, T.; Nozoye, H.; Kobayashi, N.; Kondoh, H.; Nakai, I.; Ohta, T.; Yoshimura, D.; Matsumoto, M. Effective Insulating Properties of Autooxidized Monolayers Using Organic Ditellurides. *J. Am. Chem. Soc.* **2002**, *124*, 12642−12643.
(100) Li, Y.; Silverton, L. C.; Haasch, R.; Tong, Y. Y. Alkanetelluroxide-Protected Gold Nanoparticles. *Langmuir* **2008**, *24*, 7048−7053.